Frontiers in Heat and Mass Transfer (FHMT), 11, 31 (2018)
DOI: 10.5098/hmt.11.31

Global Digital Central
ISSN: 2151-8629

Frontiers in Heat and Mass Transfer

Available at www.ThermalFluidsCentral.org

DIFFUSION-THERMO AND THERMAL-DIFFUSION EFFECTS ON RIVLIN-ERICKSEN ROTATORY CONVECTIVE FLOW PAST A POROUS VERTICAL PLATE

M. S. Dada*, S. A. Agunbiade, E. O. Titiloye

Department of Mathematics, Faculty of Physical Sciences, University of Ilorin, Nigeria

ABSTRACT

Diffusion-thermo and thermal-diffusion effects on unsteady, incompressible Rivlin-Ericksen rotatory convective flow of a magnetic conducting electrical fluid with time dependent suction between two vertical plates of which one is permeable are investigated. The uniform angular velocity rotates about an axis normal to the plate. The equations governing the flow model are non-dimensionalised, perturbed for simplification and solved by Adomian decomposition method. Graphical illustrations of the fluid parameters on velocity, temperature, concentration are presented and discussed. The effect of skin-friction, Nusselt and Sherwood numbers are presented in tabular forms and it is discovered from the results that a rise in thermal-diffusion parameter speedup the skin-friction, while increasing diffusion-thermo parameter slowdown the skin-friction.

Keywords: Diffusion-thermo, Rivlin-Ericksen fluid, Rotatory, thermal-diffusion and Unsteady.

1. INTRODUCTION

Forced and free convection mechanisms contribute significantly to heat transfer. The phenomenon occurs in both industrial and technical problems such as solar collectors, in cooling of electronic devices and nuclear reactors resulting in an emergency shutdown etc. The significance of these applications led some researchers to study natural, forced and mixed convective flows in the presence of heat and mass transfer. Deepthi and Prasada (2017) considered heat and mass transfer with mixed convective flow in the presence of radiation and Soret. In the investigation, rotatory and Dufour effects were considered insignificant. The result shown that a rise in Soret parameter decreased the heat and mass transfer rate on the walls. Soret effect on mixed convection viscoelastic fluid flow in the presence of heat and mass transfer was studied by Devasena and Ratmat (2014). The effects of Dufour and thermal radiation were not considered. Dada and Agunbiade (2016) examined the effects of chemical reaction and radiation on convective non-rotatory Rivlin-Ericksen fluid flow in a vertical porous plate. It was discovered that temperature and velocity decreased as radiation parameter increased. Aruna *et al.* (2015) investigated the influence of both thermal-diffusion and diffusion-thermo of non-rotatory mixed convective hydromagnetic fluid flow through a vertical wavy porous plate. The finite difference method was used to obtain the solution.

However, the study of rotating medium is of great importance in fluid dynamics as a result of its relevance in many natural phenomena and its applications in technology relating to Coriolis force. Some of the applications of rotating flow, particularly in porous media in the field of engineering, to mention but a few are rotating machinery, food and chemical processing industries. The study of rotating flow has gained the interest of many researchers due to its importance. Sibanda and Makinde (2010) examined steady MHD flow with heat transfer as a result of rotating disk in a porous fluid in the presence of viscous dissipation. Mutua *et al.* (2013) considered MHD free convection flow of a Newtonian fluid with variable suction through porous plate and the result revealed that skin friction increased both along x and y axes due to a decrease in rotation parameter.

In addition, Singh (2013) studied thermal radiation effects on rotatory viscoelastic MHD flow via a vertical plate. It was reported that rotation parameter enhanced velocity profiles. Oldroyd-B Rotating MHD radiative fluid through a vertical porous channel was carried out by Garg *et al.* (2014b). Guria and Jana (2013) examined rotatory viscoelastic fluid past a porous plate under a uniform suction. It was discovered that the presence of viscoelastic parameter contributed to the increase in the plate heat transfer. Abdulmaleque (2017) investigated the effects of temperature dependent suction/injection on non-Newtonian casson radiative fluid flow with viscous dissipation. Also, Garg *et al.* (2014a) presented oscillatory viscoelastic fluid flow through a porous rotating vertical channel with an assumption of an optically thin radiation and constant suction. The result showed that as the rotation parameter increased, the velocity decreased. Even though, the above investigations had contributed to the studies of fluid flow but the effects of chemical reaction was neglected in the studies and chemical reactions have tremendous impacts in changing the rate of mass diffusion.

In fluid flow that involves both heat and mass transfer, driving po-

* *Corresponding author. Email: dadamsa@gmail.com*

Global Digital Central
ISSN: 2151-8629

tentials and the fluxes relation are significantly noticed. The energy flux that is generated due to concentration gradient is referred to as diffusion-thermo, while mass flux resulting from temperature gradients is thermal-diffusion. Mostly, the effects of diffusion-thermo and thermal-diffusion are often neglected in most studies on the bases that they are of low magnitude in relation to the rest chemical species. The effects of Dufour and Soret become significant phenomena in areas like petrology, hydrology, geosciences, etc. The effect of thermal-diffusion is relevant, for example, in the separation of isotope and mixture of gases that has light molecular weight. Therefore, Sarma and Govardhan (2016) reported on the effects of thermal-diffusion and diffusion-thermo on natural convection heat and mass transfer with thermal radiation in the presence of viscous dissipation in a porous medium. A Newtonian fluid was examined in the study and finite difference method was used in the computations of the results. It was reported that velocity profiles was accelerated by increase in viscous dissipation. The effects of thermal-diffusion and diffusion-thermo on free convection MHD flow of Rivlin-Ericksen fluid was examined by Reddy *et al.* (2016). Rotatory and thermal radiation effects were considered to be insignificant, the result shown that an increase in diffusion-thermo and thermal-diffusion speedup the skin-friction. Gbadeyan *et al.* (2011) examined the influence of Soret and Dufour with heat and mass transfer on mixed convective viscoelastic fluid flow past a porous medium. It was observed from the result that Soret enhanced both concentration and temperature profiles.

Furthermore, Dada and Salawu (2017) presented heat and mass transfer of pressure-driven flow with inclined magnetic field. The result revealed that an increase in chemical reaction reduced both pressure and concentration profiles. Ibrahim and Suneetha (2015) studied effects of Soret and chemical reaction on MHD unsteady viscoelastic fluid past an infinite vertical plate. The study concluded that both concentration and velocity profiles increased as thermal-diffusion increased. Hayat *et al.* (2017) investigated Dufour and Soret effects on MHD Jeffrey fluid of peristaltic transport in a curved channel. It was observed that Dufour and Soret have opposite behaviour for concentration and temperature. Babu *et al.* (2017) considered diffusion-thermo and thermal-diffusion effects on heat and mass transfer MHD Jeffery fluid flow in a stretching sheet. The result revealed that temperature profiles was reduced by an increase in either Prandtl number or Soret parameter. Influence of thermal-diffusion on Kurshinshiki fluid in the presence of heat and mass transfer past a vertical porous plate was investigated by Jimoh *et al.* (2014). At the boundary layer, the result shown that increase in the heat sources parameter improved both velocity and temperature profiles. However, as impressive as the above studies were, rotatory Rivlin-Ericksen fluid flows have received no significant attention.

A careful examination of all the above studies on heat and mass transfer showed that combined effects of time dependence suction, pressure gradient and heat absorption in Rivlin-Ericksen convective fluid flow in a rotating medium with diffusion-thermo and thermal-diffusion have received little or no attention. Considering various phenomena, combined effects of all these parameters come into consideration in a practical flows of fluid and are of practical applications in the field of engineering, chemical processing industry, rotating machinery, paper and food processing industry, petroleum industry and other areas that involve viscoelastic fluid flow. Hence, this present study analyses the effects of diffusion-thermo, thermal-diffusion and radiation effects on convective Rivlin-Ericksen fluid in a rotating system with chemical reaction.

2. MATHEMATICAL ANALYSIS

Consider a non-Newtonian, two-dimensional incompressible free convective Rivlin-Ericksen flow of an electrically conducting fluid through a rotating vertical channel with a periodic suction. The following assumptions are made in the formulation of this problem:

(i) an unsteady and laminar flow is considered;

(ii) induced magnetic field and Hall effects are ignored due to the fact that magnetic Reynolds number and transversely applied magnetic field is considered to be very small;

(iii) a magnetic field (B_0) of uniform strength is perpendicularly applied to the plates;

(iv) there is a rotation of the entire system through the perpendicular axis to the plates;

(v) thermal-diffusion and diffusion-thermo are assumed to be of substantial magnitude, hence, they are not negligible;

(vi) the plates are considered to be infinite in x^*-direction, hence all physical quantities excluding pressure are functions of coordinate z^* and time t^*;

(vii) in the flow field, pressure is taken to be constant; and

(viii) the fluid is finitely conducting with constant physical properties.

With the above assumptions, the flow chart and governing equations are as follows:

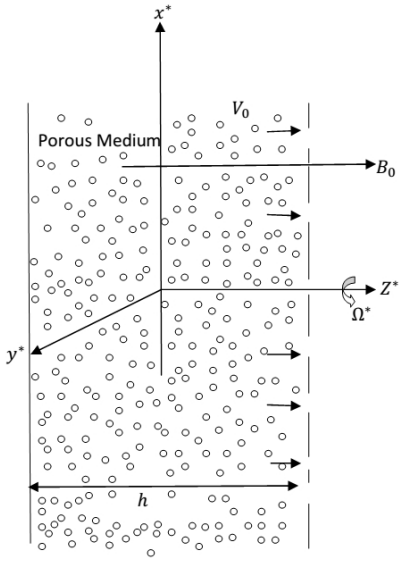

Fig. 1 Physical Configuration of the flow

$$\frac{\partial w^*}{\partial z^*} = 0 \tag{1}$$

$$\frac{\partial u^*}{\partial t^*} + \nu^* \frac{\partial u^*}{\partial z^*} = -\frac{1}{\rho}\frac{\partial p^*}{\partial x^*} + \nu \frac{\partial^2 u^*}{\partial z^{*2}} + 2\Omega^* v^* + g\beta_T \left(T^* - T_h^*\right) + g\beta_C \left(C^* - C_h^*\right) - \nu \frac{u^*}{k_p^*} - \frac{\sigma B_o^2 u^*}{\rho} - \beta_1 \left(\frac{\partial^3 u^*}{\partial t^* \partial z^{*2}} + \nu^* \frac{\partial^3 u^*}{\partial z^{*3}}\right) \tag{2}$$

$$\frac{\partial v^*}{\partial t^*} + \nu^* \frac{\partial v^*}{\partial z^*} = -\frac{1}{\rho}\frac{\partial p^*}{\partial y^*} + \nu \frac{\partial^2 v^*}{\partial z^{*2}} - 2\Omega^* u^* - \nu \frac{v^*}{k_p^*} - \frac{\sigma B_o^2 v^*}{\rho} - \beta_1 \left(\frac{\partial^3 v^*}{\partial t^* \partial z^{*2}} + \nu^* \frac{\partial^3 v^*}{\partial z^{*3}}\right) \tag{3}$$

Global Digital Central
ISSN: 2151-8629

$$\frac{\partial T^*}{\partial t^*}+\nu^*\frac{\partial T^*}{\partial z^*}= \alpha\frac{\partial^2 T^*}{\partial z^{*2}}-\frac{\phi_0}{\rho c_p}\left(T^*-T_h^*\right)- \frac{1}{\rho C_p}\frac{\partial q_R}{\partial z^*}+\frac{Dk_T\partial^2 C^*}{C_pC_s\partial z^{*2}} \quad (4)$$

$$\frac{\partial C^*}{\partial t^*}+\nu^*\frac{\partial C^*}{\partial z^*}=D\frac{\partial^2 C^*}{\partial z^{*2}}-K_1^*\left(C^*-C_h^*\right)+\frac{DK_T}{T_m}\frac{\partial^2 T^*}{\partial z^{*2}} \quad (5)$$

The boundary conditions for the problem are:

$$\left.\begin{array}{l} z^*=0; u^*=v^*=0, T^*=T_0^*+\epsilon\left(T_0^*-T_h^*\right)\cos\varpi^* t^*, \\ C^*=C_0^*+\epsilon\left(C_0^*-C_h^*\right)\cos w^* t^* \\ z^*=h;\ \ u^*=W_o\left(1+\epsilon\cos\varpi^* t^*\right),\ \ v^*=0, \\ T^*=T_h^*,\ \ C^*=C_h^* \end{array}\right\} \quad (6)$$

The time dependent suction velocity is expressed in exponential form as:
$\nu^*=-W_o\left(1+\epsilon Ae^{i\varpi^* t^*}\right)$ (Das *et al.* (2011)), ϵ and ϵA is small values less than unity. q_R is the radiative heat flux and is defined base on Rosseland approximation (Brewster (1972)) as:

$$q_R = -\frac{4\sigma}{3k^1}\frac{\partial T^{*4}}{\partial z^*} \quad (7)$$

This present analysis is limited to optically thick fluid, hence Rosseland approximation is used. Considering the temperature differences within the flow to be sufficiently small, T^{*4} (quartic temperature function) can be expanded using Taylor series expansion and neglecting higher order terms gives;

$$T^{*4}\approx 4T_h^{*3}T^*-3T_h^{*4} \quad (8)$$

This is substituted into radiative heat flux term that was used in Eq. (4). The pressure gradient for the fluid is considered in the form;

$$-\frac{1}{\rho}\frac{\partial P^*}{\partial y^*}=0 \quad and \quad -\frac{1}{\rho}\frac{\partial P^*}{\partial x^*}=H\epsilon cos\varpi t \quad (9)$$

where H is a constant and it oscillates only in x-axis direction.

The accompanying non-dimensional variables are utilized to reduce the governing equations to non-dimensional form.

$$\left.\begin{array}{l} \xi=\frac{u^*}{W_o}, v=\frac{v^*}{W_o}, t=\frac{t^*W_o^2}{\nu}, \eta=\frac{W_o z^*}{\nu}=\frac{z^*}{h}, \\ \vartheta=\frac{T^*-T_h^*}{T_0^*-T_h^*},\ \varpi=\frac{\varpi^*\nu}{W_o^2}, P_r=\frac{\nu\rho C_p}{k_p}=\frac{\nu}{\alpha}, x=\frac{W_o x^*}{\nu} \\ M=\frac{\sigma B_0^2\nu}{\rho W_o^2}, G_h=\frac{\nu g\beta_T(T_0^*-T_h^*)}{W_o^3}, S_C=\frac{\nu}{D}, V_R=\frac{\beta_1 W_o^2}{\nu^2} \\ G_m=\frac{\nu g\beta_c(C_0^*-C_h^*)}{W_o^3}, y=\frac{W_o y^*}{\nu}, P=\frac{P^*}{\rho W_o^2}, \zeta=\frac{C^*-C_h^*}{C_0^*-C_h^*} \\ E=\frac{k^1 k_p}{4\sigma T_h^{*3}}, \Omega=\frac{\Omega^*\nu}{W_o^2}, K_r=\frac{K_1\nu}{W_o^2}, \phi=\frac{\nu\phi_0}{\rho C_p W_o^2} \\ S_p=\frac{DK_T(T_0^*-T_h^*)}{\nu T_m(C_0^*-C_h^*)}, D_p=\frac{DK_T(C_0^*-C_h^*)}{C_sC_p\nu(T_0^*-T_h^*)}, k_p=\frac{k_p^* W_o^2}{\nu^2} \end{array}\right\} \quad (10)$$

By applying non-dimensional variables (10), Eqs (2)-(5) become

$$\frac{\partial\xi}{\partial t}-\left(1+\epsilon Ae^{i\varpi t}\right)\frac{\partial\xi}{\partial\eta}=H\epsilon cos\varpi t+\frac{\partial^2\xi}{\partial\eta^2}+2\Omega v+G_h\vartheta- \left(M+\frac{1}{k_p}\right)\xi+G_m\zeta-V_R\left(\frac{\partial^3\xi}{\partial t\partial\eta^2}-\left(1+\epsilon Ae^{i\varpi t}\right)\frac{\partial^3\xi}{\partial\eta^3}\right) \quad (11)$$

$$\frac{\partial v}{\partial t}-\left(1+\epsilon Ae^{i\varpi t}\right)\frac{\partial v}{\partial\eta}=\frac{\partial^2 v}{\partial\eta^2}-2\Omega\xi-\left(M+\frac{1}{k_p}\right)v - V_R\left(\frac{\partial^3 v}{\partial t\partial\eta^2}-\left(1+\epsilon Ae^{i\varpi t}\right)\frac{\partial^3 v}{\partial\eta^3}\right) \quad (12)$$

$$\frac{\partial\vartheta}{\partial t}-\left(1+\epsilon Ae^{i\varpi t}\right)\frac{\partial\vartheta}{\partial\eta}=\left(\frac{1}{P_r}+\frac{4}{3EP_r}\right)\frac{\partial^2\vartheta}{\partial\eta^2} -\phi\vartheta+D_p\frac{\partial^2\zeta}{\partial\eta^2} \quad (13)$$

$$\frac{\partial\zeta}{\partial t}-\left(1+\epsilon Ae^{i\varpi t}\right)\frac{\partial\zeta}{\partial\eta}=\frac{1}{S_c}\frac{\partial^2\zeta}{\partial\eta^2}-K_r\zeta+S_p\frac{\partial^2\vartheta}{\partial\eta^2} \quad (14)$$

The boundary conditions are:

$$\left.\begin{array}{l} \psi=0,\ \vartheta=1+\frac{\epsilon}{2}\left(e^{i\varpi t}+e^{-i\varpi t}\right), \\ \zeta=1+\frac{\epsilon}{2}\left(e^{i\varpi t}+e^{-i\varpi t}\right)\ at\ \eta=0 \\ \psi=1+\frac{\epsilon}{2}\left(e^{i\varpi t}+e^{-i\varpi t}\right),\ \vartheta=0\ ,\ \zeta=0\ at\ \eta=1 \end{array}\right\} \quad (15)$$

where ξ, ϑ, ζ, η, Ω, R_v, E, k_r, M, Pr, Sc, ϕ, V_R, A, D_p, S_p, G_h , G_m are velocity, temperature, concentration, plates distance apart, rotation parameter, resultant velocity, radiation parameter, chemical reaction parameter, magnetic parameter, Prandtl number, Schmidt number, heat absorption coefficient, viscoelasticity parameter, suction velocity parameter, Dufour number, Thermal-diffusion parameter, Grashof number for heat and mass transfer, respectively.
Taking $\psi=\xi+iv$ then, Eqs (11) and (12) combine to

$$\frac{\partial\psi}{\partial t}-\left(1+\epsilon Ae^{i\varpi t}\right)\frac{\partial\psi}{\partial\eta}=H\epsilon cos\varpi t+\frac{\partial^2\psi}{\partial\eta^2}-(2i\Omega+F)\psi+G_h\vartheta+ G_m\zeta-V_R\left(\frac{\partial^3\psi}{\partial t\partial\eta^2}-\left(1+\epsilon Ae^{i\varpi t}\right)\frac{\partial^3\psi}{\partial\eta^3}\right) \quad (16)$$

where

$$F=M+\frac{1}{k_P}$$

3. METHOD OF SOLUTION

3.1. Perturbation method

The partial differential Eqs. (13), (14) and (16) are reduced to ordinary differential equations by Perturbation technique. Due to the nature of the boundary conditions, the assumed solutions can be written as follows.(Garg *et al.* (2014b))

$$\left.\begin{array}{l} \psi(\eta,t)=\psi_0(\eta)+\frac{\epsilon}{2}\left(\psi_1(\eta)e^{i\varpi t}+\psi_2(\eta)e^{-i\varpi t}\right) \\ \vartheta(\eta,t)=\vartheta_0(\eta)+\frac{\epsilon}{2}\left(\vartheta_1(\eta)e^{i\varpi t}+\vartheta_2(\eta)e^{-i\varpi t}\right) \\ \zeta(\eta,t)=\zeta_0(\eta)+\frac{\epsilon}{2}\left(\zeta_1(\eta)e^{i\varpi t}+\zeta_2(\eta)e^{-i\varpi t}\right) \end{array}\right\} \quad (17)$$

Substituting equation (17) into Eqs. (13), (14) and (16) gives:

$$V_R\psi_0'''+\psi_0''+\psi_0'-(2i\Omega+F)\psi_0=-G_h\vartheta_0-G_m\zeta_0 \quad (18)$$

$$V_R\psi_1'''+(1-V_Ri\varpi)\psi_1''+\psi_1'-(i\varpi+2i\Omega+F)\psi_1=-H- 2A\psi_0'-G_h\vartheta_1-G_m\zeta_1-2V_RA\psi_0''' \quad (19)$$

$$V_R\psi_2'''+(1+V_Ri\varpi)\psi_2''+\psi_2'-(2i\Omega+F-i\varpi)\psi_2=-H- G_h\vartheta_2-G_m\zeta_2 \quad (20)$$

$$B\vartheta_0''+\vartheta_0'-\phi\vartheta_0=-D_p\zeta_o'' \quad (21)$$

$$B\vartheta_1''+\vartheta_1'-(\phi+i\varpi)\vartheta_1=-2A\vartheta_0'-D_p\zeta_1'' \quad (22)$$

$$B\vartheta_2''+\vartheta_2'-(\phi-i\varpi)\vartheta_2=-D_p\zeta_2'' \quad (23)$$

$$\zeta_0''+S_c\zeta_0'-S_cK_r\zeta_0=-S_cS_p\vartheta_0'' \quad (24)$$

$$\zeta_1''+S_c\zeta_1'-S_c\left(K_r+i\varpi\right)\zeta_1=-2AS_c\zeta_0'-S_cS_p\vartheta_1'' \quad (25)$$

$$\zeta_2''+S_c\zeta_2'-S_c\left(K_r-i\varpi\right)\zeta_2=-S_cS_p\vartheta_2'' \quad (26)$$

where

$$B=\frac{1}{P_r}+\frac{4}{3EP_r}$$

The boundary conditions for the problem are:

$$\left.\begin{array}{l} \psi_0=\psi_1=\psi_2=0,\ \vartheta_0=\vartheta_1=\vartheta_2=1, \\ \zeta_0=\zeta_1=\zeta_2=1\ at\ \eta=0 \\ \psi_0=\psi_1=\psi_2=1,\ \vartheta_0=\vartheta_1=\vartheta_2=0, \\ \zeta_0=\zeta_1=\zeta_2=0\ at\ \eta=1 \end{array}\right\} \quad (27)$$

Global Digital Central
ISSN: 2151-8629

Equations (18)-(20) are third order differential equations with only two boundary conditions. In order to obtain necessary and sufficient boundary conditions (Beard and Walters (1964)) and (Garg *et al.* (2014b)), the solutions are expressed in the forms:

$$\left.\begin{array}{l}\psi_0(\eta)=\psi_{01}(\eta)+V_R\psi_{02}(\eta)+0(V_R^2)\\ \psi_1(\eta)=\psi_{11}(\eta)+V_R\psi_{12}(\eta)+0(V_R^2)\\ \psi_2(\eta)=\psi_{21}(\eta)+V_R\psi_{22}(\eta)+0(V_R^2)\\ \vartheta_0(\eta)=\vartheta_{01}(\eta)+V_R\vartheta_{02}(\eta)+0(V_R^2)\\ \vartheta_1(\eta)=\vartheta_{11}(\eta)+V_R\vartheta_{12}(\eta)+0(V_R^2)\\ \vartheta_2(\eta)=\vartheta_{21}(\eta)+V_R\vartheta_{22}(\eta)+0(V_R^2)\\ \zeta_0(\eta)=\zeta_{01}(\eta)+V_R\zeta_{02}(\eta)+0(V_R^2)\\ \zeta_1(\eta)=\zeta_{11}(\eta)+V_R\zeta_{12}(\eta)+0(V_R^2)\\ \zeta_2(\eta)=\zeta_{21}(\eta)+V_R\zeta_{22}(\eta)+0(V_R^2)\end{array}\right\} \quad (28)$$

Applying Eqs. (28) to Eqs. (18)-(26) gives:

$$\psi_{01}''+\psi_{01}'-(2i\Omega+F)\,\psi_{01}=-G_h\vartheta_{01}-G_m\zeta_{01} \quad (29)$$

$$\psi_{02}''+\psi_{02}'-(2i\Omega+F)\,\psi_{02}=-\psi_{01}'''-G_h\vartheta_{02}-G_m\zeta_{02} \quad (30)$$

$$\psi_{11}''+\psi_{11}'-(i\varpi+2i\Omega+F)\,\psi_{11}=-H-2A\psi_{01}'-G_h\vartheta_{11}-G_m\zeta_{11} \quad (31)$$

$$\psi_{12}''+\psi_{12}'-(i\varpi+2i\Omega+F)\,\psi_{12}=i\varpi\psi_{11}''-\psi_{11}'''-2A\psi_{02}'-2A\psi_{01}'''-G_h\vartheta_{12}-G_m\zeta_{12} \quad (32)$$

$$\psi_{21}''+\psi_{21}'-(2i\Omega+F-i\varpi)\,\psi_{21}=-H-G_h\vartheta_{21}-G_m\zeta_{21} \quad (33)$$

$$\psi_{22}''+\psi_{22}'-(2i\Omega+F-i\varpi)\,\psi_{22}=-\psi_{21}'''-i\varpi\psi_{21}''-G_h\vartheta_{22}-G_m\zeta_{22} \quad (34)$$

$$B\vartheta_{01}''+\vartheta_{01}'-\phi\vartheta_{01}=-D_p\zeta_{01}'' \quad (35)$$

$$B\vartheta_{02}''+\vartheta_{02}'-\phi\vartheta_{02}=-D_p\zeta_{02}'' \quad (36)$$

$$B\vartheta_{11}''+\vartheta_{11}'-(\phi+i\varpi)\,\vartheta_{11}=-2A\vartheta_{01}'-D_p\zeta_{11}'' \quad (37)$$

$$B\vartheta_{12}''+\vartheta_{12}'-(\phi+i\varpi)\,\vartheta_{12}=-2A\vartheta_{02}'-D_p\zeta_{12}'' \quad (38)$$

$$B\vartheta_{21}''+\vartheta_{21}'-(\phi-i\varpi)\,\vartheta_{21}=-D_p\zeta_{21}'' \quad (39)$$

$$B\vartheta_{22}''+\vartheta_{22}'-(\phi-i\varpi)\,\vartheta_{22}=-D_p\zeta_{22}'' \quad (40)$$

$$\zeta_{01}''+S_c\zeta_{01}'-S_cK_r\zeta_{01}=-S_cS_p\vartheta_{01}'' \quad (41)$$

$$\zeta_{02}''+S_c\zeta_{02}'-S_cK_r\zeta_{02}=-S_cS_p\vartheta_{02}'' \quad (42)$$

$$\zeta_{11}''+S_c\zeta_{11}'-S_c(K_r+i\varpi)\zeta_{11}=-2AS_c\zeta_{01}'-S_cS_p\vartheta_{11}'' \quad (43)$$

$$\zeta_{12}''+S_c\zeta_{12}'-S_c(K_r+i\varpi)\zeta_{12}=-2AS_c\zeta_{02}'-S_cS_p\vartheta_{12}'' \quad (44)$$

$$\zeta_{21}''+S_c\zeta_{21}'-S_c\,(K_r-i\varpi)\,\zeta_{21}=-S_cS_p\vartheta_{21}'' \quad (45)$$

$$\zeta_{22}''+S_c\zeta_{22}'-S_c\,(K_r-i\varpi)\,\zeta_{22}=-S_cS_p\vartheta_{22}'' \quad (46)$$

subject to the following boundary conditions:

$$\left.\begin{array}{l}\psi_{01}=\psi_{02}=\psi_{11}=\psi_{12}=\psi_{21}=\psi_{22}=0\ \ at\ \ \eta=0\\ \psi_{01}=\psi_{11}=\psi_{21}=1,\ \ \psi_{02}=\psi_{12}=\psi_{22}=0\ \ at\ \ \eta=1\\ \vartheta_{01}=\vartheta_{11}=\vartheta_{21}=1,\ \ \vartheta_{02}=\vartheta_{12}=\vartheta_{22}=0\ \ at\ \ \eta=0\\ \vartheta_{01}=\vartheta_{11}=\vartheta_{21}=0,\ \ \vartheta_{02}=\vartheta_{12}=\vartheta_{22}=0\ \ at\ \ \eta=1\\ \zeta_{01}=\zeta_{11}=\zeta_{21}=1,\ \ \zeta_{02}=\zeta_{12}=\zeta_{22}=0\ \ at\ \ \eta=0\\ \zeta_{01}=\zeta_{11}=\zeta_{21}=0,\ \ \zeta_{02}=\zeta_{12}=\zeta_{22}=0\ \ at\ \ \eta=1\end{array}\right\} \quad (47)$$

3.2. Adomian Decomposition method

The ordinary differential Eqs. (29)-(46), though linear but are highly coupled, hence Adomian decomposition methods is applied in solving the problem. A differential equation can be written in a general form as;

$$F\psi(\eta)=b \quad (48)$$

where F represents an operator of nonlinear ordinary differential equation containing both linear and nonlinear terms. $L\psi$ represents the linear term, and the invertible linear operator is L. Taking the highest-ordered derivative as L, L^{-1} is n-fold integration operator from 0 to η for $L=\frac{d^n}{d\eta^n}$. For the linear operator L, the remainder is R and $N\psi$ is the nonlinear term. Hence,

$$L\psi+R\psi+N\psi=b \quad (49)$$

$$L\psi=b-R\psi-N\psi \quad (50)$$

Since L is invertible, thus

$$L^{-1}L\psi=L^{-1}b-L^{-1}R\psi-L^{-1}N\psi \quad (51)$$

The highest-order in Equations (29)-(46) is two, therefore,

$$L^{-1}L\psi=\int_0^\eta\int_0^s\psi''(\eta)d\eta ds \quad (52)$$

$$L^{-1}L\psi=\psi-\psi(0)-\eta\psi'(0) \quad (53)$$

substituting for $L^{-1}L\psi$ in Equation (51), the equation becomes;

$$\psi=\psi(0)+\eta\psi'(0)+L^{-1}b-L^{-1}R\psi-L^{-1}N\psi \quad (54)$$

Hence,

$$\psi=\psi(0)+\eta\psi'(0)+b\frac{\eta^2}{2}-\int_0^\eta\int_0^s(R\psi+N\psi)\,d\eta ds \quad (55)$$

ψ can be written in series form as:

$$\psi=\sum_{n=0}^{\infty}\psi_n \quad (56)$$

also, the nonlinear term as:

$$N\psi=\sum_{n=0}^{\infty}A_n \quad (57)$$

where

$$A_n=\frac{1}{n!}\frac{d^n}{d\lambda^n}\left(F\left(\sum_{i=0}^{n}\lambda^i\psi_i\right)\right)_{\lambda=0}\qquad n=0,1,2,3,... \quad (58)$$

Substituting Equations (56) and (57) into equation (55) gives;

$$\sum_{n=0}^{\infty}\psi_n=\psi(0)+\eta\psi'(0)+b\frac{\eta^2}{2}-\int_0^\eta\int_0^s\left(R\sum_{n=0}^{\infty}\psi_n+\sum_{n=0}^{\infty}A_n\right)d\eta ds \quad (59)$$

The first three terms are identified as ψ_0 which is the initial approximation, that is

$$\psi_0=\psi(0)+\eta\psi'(0)+b\frac{\eta^2}{2} \quad (60)$$

and

$$\psi_{n+1}=-\int_0^\eta\int_0^s\left(R\sum_{n=0}^{\infty}\psi_n+\sum_{n=0}^{\infty}A_n\right)d\eta ds \quad (61)$$

Global Digital Central
ISSN: 2151-8629

is the recurrence relation. All the components can be determined since A_0 depends on ψ_0 only, A_1 depends on ψ_0 and ψ_1 and so on. The solution then is the n-term approximation or approximant to ψ.

From Eqs. (60) and (61), the approximate solutions for Eqs (29)-(46), which converges at $n = 5$, can be written as:

$$\left.\begin{array}{l}\zeta_{01} = \sum_{a=0}^{5}\zeta_{01}[a],\ \vartheta_{01} = \sum_{a=0}^{5}\vartheta_{01}[a];\\ \psi_{01} = \sum_{a=0}^{5}\psi_{01}[a], \zeta_{02} = \sum_{a=0}^{5}\zeta_{02}[a],\\ \vartheta_{02} = \sum_{a=0}^{5}\vartheta_{02}[a];\ \psi_{02} = \sum_{a=0}^{5}\psi_{02}[a],\\ \zeta_{11} = \sum_{a=0}^{5}\zeta_{11}[a],\ \vartheta_{11} = \sum_{a=0}^{5}\vartheta_{11}[a];\\ \psi_{11} = \sum_{a=0}^{5}\psi_{11}[a], \zeta_{12} = \sum_{a=0}^{5}\zeta_{12}[a],\\ \vartheta_{12} = \sum_{a=0}^{5}\vartheta_{12}[a];\ \psi_{12} = \sum_{a=0}^{5}\psi_{12}[a],\\ \zeta_{21} = \sum_{a=0}^{5}\zeta_{21}[a],\ \vartheta_{21} = \sum_{a=0}^{5}\vartheta_{21}[a];\\ \psi_{21} = \sum_{a=0}^{5}\psi_{21}[a], \zeta_{22} = \sum_{a=0}^{5}\zeta_{22}[a],\\ \vartheta_{22} = \sum_{a=0}^{5}\vartheta_{22}[a];\ \psi_{22} = \sum_{a=0}^{5}\psi_{22}[a]\end{array}\right\} \quad (62)$$

Series solutions (62) are substituted in Eqs. (17) and (28) to give the final solution for velocity, temperature and concentration distributions

$$\psi(\eta,t) = \sum_{a=0}^{5}\psi_{01}[a](\eta) + V_R\sum_{a=0}^{5}\psi_{02}[a](\eta) + \frac{\epsilon}{2}\left(\left(\sum_{a=0}^{5}\psi_{11}[a](\eta) + V_R\sum_{a=0}^{5}\psi_{12}[a](\eta)\right)e^{i\varpi t} + \left(\sum_{a=0}^{5}\psi_{21}[a](\eta) + V_R\sum_{a=0}^{5}\psi_{22}[a](\eta)\right)e^{-i\varpi t}\right) \quad (63)$$

$$\vartheta(\eta,t) = \sum_{a=0}^{5}\vartheta_{01}[a](\eta) + V_R\sum_{a=0}^{5}\vartheta_{02}[a](\eta) + \frac{\epsilon}{2}\left(\left(\sum_{a=0}^{5}\vartheta_{11}[a](\eta) + V_R\sum_{a=0}^{5}\vartheta_{12}[a](\eta)\right)e^{i\varpi t} + \left(\sum_{a=0}^{5}\vartheta_{21}[a](\eta) + V_R\sum_{a=0}^{5}\vartheta_{22}[a](\eta)\right)e^{-i\varpi t}\right) \quad (64)$$

$$\zeta(\eta,t) = \sum_{a=0}^{5}\zeta_{01}[a](\eta) + V_R\sum_{a=0}^{5}\zeta_{02}[a](\eta) + \frac{\epsilon}{2}\left(\left(\sum_{a=0}^{5}\zeta_{11}[a](\eta) + V_R\sum_{a=0}^{5}\zeta_{12}[a](\eta)\right)e^{i\varpi t} + \left(\sum_{a=0}^{5}\zeta_{21}[a](\eta) + V_R\sum_{a=0}^{5}\zeta_{22}[a](\eta)\right)e^{-i\varpi t}\right) \quad (65)$$

3.3. Skin-friction, Nusselt and Sherwood number in term of Amplitude

With reference to the boundary conditions, the amplitude is defined in terms of primary and secondary velocities for steady and unsteady flow. Therefore, total resultant velocity can be written as;

$$R_v = \sqrt{d^2 + f^2} \quad (66)$$

where velocity is defined as

$$\psi(\eta,t) = d + if \quad (67)$$

The Skin-friction is given as;

$$\tau(\eta) = \left(\frac{\partial\psi}{\partial\eta}\right)_{\eta=0,1} = \tau_m + i\tau_n \quad (68)$$

$$\beta_1 = \sqrt{\tau_m^2 + \tau_n^2} \quad (69)$$

Nusselt number (Heat transfer coefficient) is defined as;

$$Nu(\eta) = -\left(1 + \frac{4}{3E}\right)\left(\frac{\partial\vartheta}{\partial\eta}\right)_{\eta=0,1} = \beta_m + i\beta_n \quad (70)$$

$$\beta_2 = \sqrt{\beta_m^2 + \beta_n^2} \quad (71)$$

Sherwood Number(Mass transfer coefficient) is expressed as:

$$Sh(\eta) = \left(\frac{\partial\zeta}{\partial\eta}\right)_{\eta=0,1} = \lambda_m + i\lambda_n \quad (72)$$

$$\beta_3 = \sqrt{\lambda_m^2 + \lambda_n^2} \quad (73)$$

4. DISCUSSION OF RESULTS

The solutions for the partial differential equations (13), (14) and (16) with the corresponding boundary conditions (15) are acquired by Adomian decomposition methods alongside with MATHEMATICA programming. The impacts of different parameters governing the flow field on velocity, temperature and species in the fliud are depicted in tabular and graphical forms. The parameters considered in this study include: dimensionless viscoelasticity parameter of the Rivlin-Ericksen fluid (V_R), suction velocity parameter (A), rotation parameter (Ω), scalar constant (ϵ), chemical reaction parameter (K_r), thermal radiation parameter (E), Prandtl number (P_r), Schmidt number (S_c), heat absorption coefficient (ϕ), Mass transfer Grashof number (G_m), Heat transfer Grashof number (G_h), permeability of the porous medium (k_p), Dufour parameter (D_p), Soret parameter (S_p) and magnetic parameter (M). Throughout the computations, the following are taken as default values: $t = 1$, $G_h = G_m = M = 5$, $V_R = 0.05$, $\phi = 0.005$, $P_r = 0.71$, $E = 3$, $\epsilon = 0.01$, $A = k_p = 0.5$, $K_r = 2$, $\Omega = 10$, $D_p = 0.1$, $S_p = 2$ and $S_c = 1.002$.

Figures 2 and 3 depict the effects of Suction velocity parameter (A) on concentration and resultant velocity (R_v). It is obvious that as Suction velocity parameter increases, resultant velocity and concentration increase.

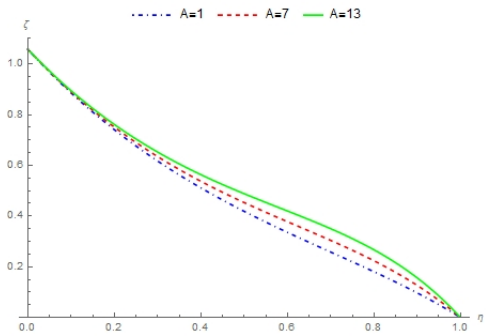

Fig. 2 Variation of dimensionless concentration ζ with suction velocity parameter A

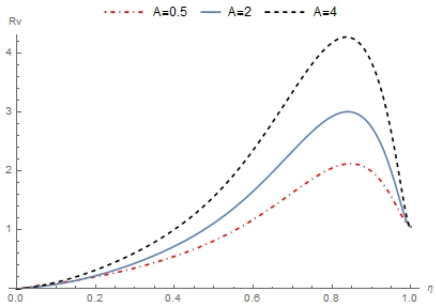

Fig. 3 Variation of resultant velocity R_v with suction velocity parameter A

Variation of values of scalar constant (ϵ) on resultant velocity, temperature and species distribution is shown in Figs. 4 - 6. It is detected that increasing ϵ causes a corresponding increment on resultant velocity, temperature and species profiles.

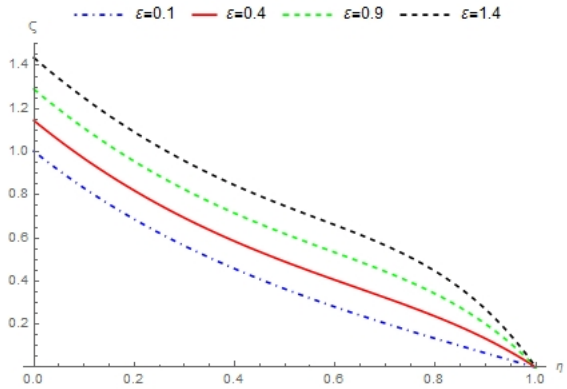

Fig. 4 Variation of dimensionless concentration ζ with scalar constant ϵ

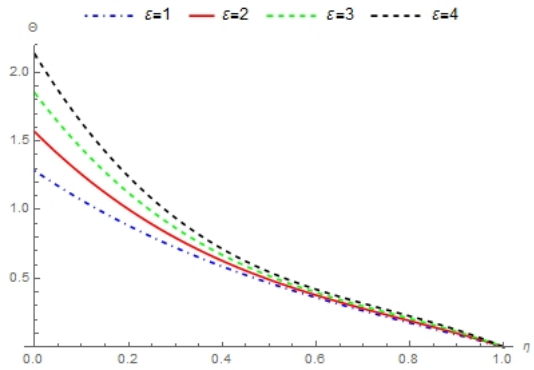

Fig. 5 Variation of dimensionless temperature ϑ with scalar constant ϵ

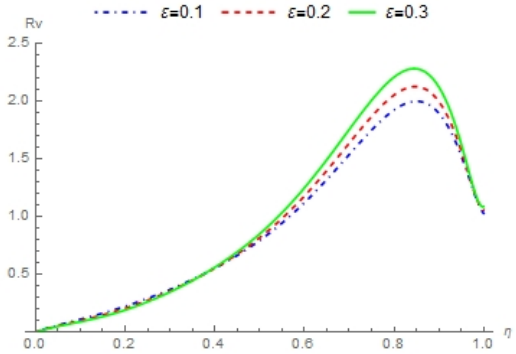

Fig. 6 Variation of resultant velocity R_v with scalar constant ϵ

The influence of G_m, G_h and k_p on velocity is illustrated in Figs. 7 - 9. From these Figures, resultant velocity is enhanced by an increase in G_m, G_h and k_p.

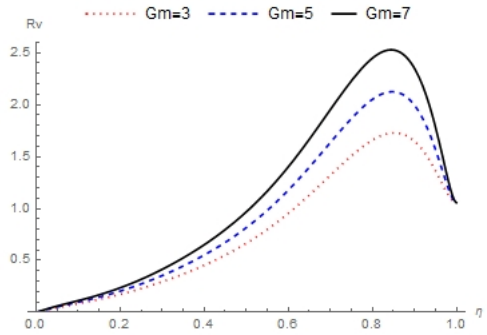

Fig. 7 Variation of resultant velocity R_v with mass transfer Grashof number Gm

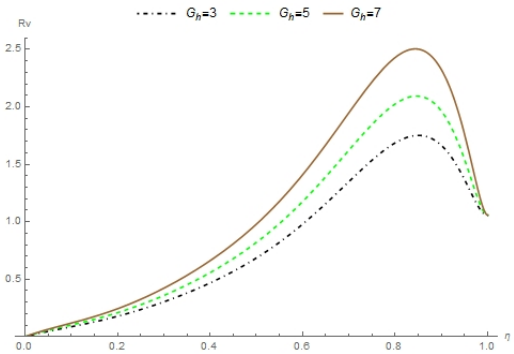

Fig. 8 Variation of resultant velocity R_v with heat transfer Grashof number G_h

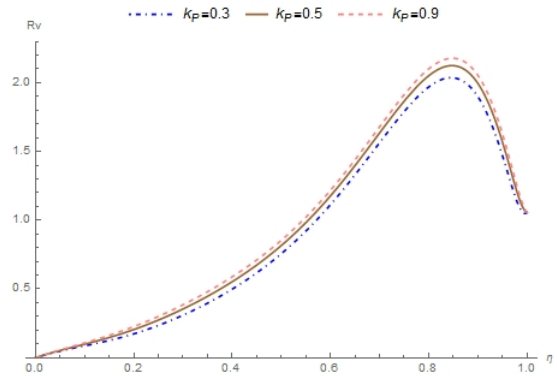

Fig. 9 Variation of resultant velocity R_v with permeability of the porous medium k_p

Figures 10 and 11 display the effect of the different values of K_r on species and velocity profiles. It is observed that the more the value of K_r, the less the species and resultant velocity.

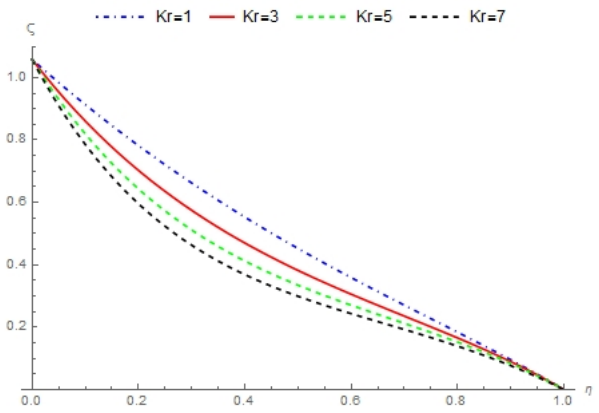

Fig. 10 Variation of dimensionless concentration ζ with chemical reaction parameter Kr

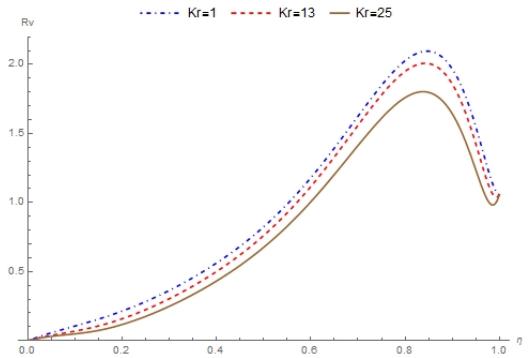

Fig. 11 Variation of resultant velocity R_v with chemical reaction parameter Kr

Figure 12 reveals the influence of M on the resultant velocity. It is clear from the figure that a higher value of M decreases the flow velocity throughout the domain of the fluid. A drag force identified as Lorentz force is produced in electrically conducting fluid where magnetic field is applied. There is a decrease in the velocity of the fluid as a result of the effect of this drag force since fluid transport is resisted in the presence of the magnetic field.

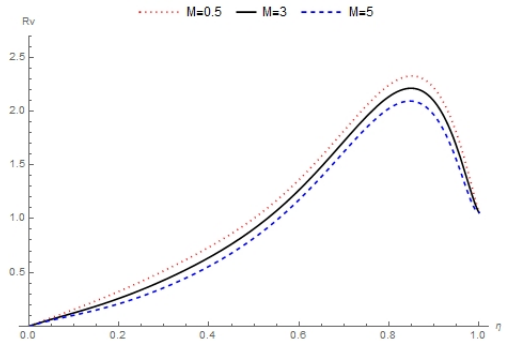

Fig. 12 Variation of resultant velocity R_v with magnetic parameter M

The contribution of radiation parameter is represented in Figs. 13 and 14. From these figures, it is shown a rise in E slows temperature distribution down. However, resultant velocity distribution is improved with a rise in E. This result revealed that higher values of radiation parameter are equivalent to increasing dominance conduction over E. Hence, there is reduction in buoyancy force and temperature in the thermal boundary layer.

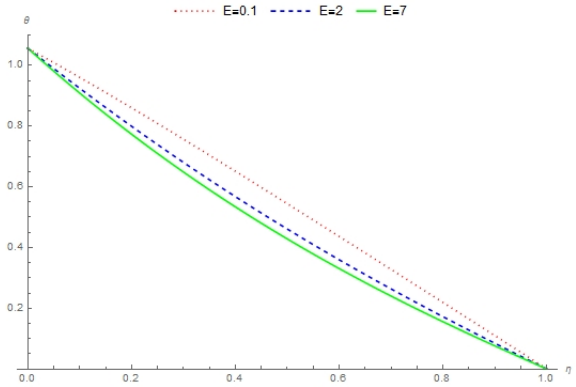

Fig. 13 Variation of dimensionless temperature ϑ with thermal radiation parameter E

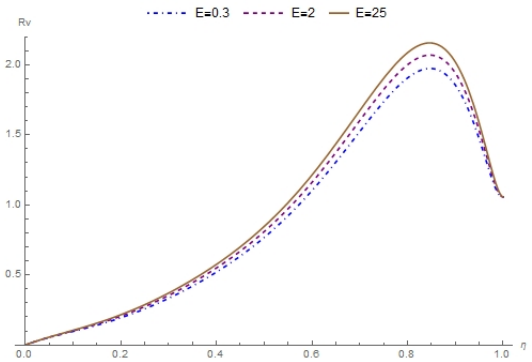

Fig. 14 Variation of resultant velocity R_v with thermal radiation parameter E

The effect of Ω on resultant velocity is seen in Fig. 15. The result revealed that, higher values of rotation parameter enhanced resultant velocity profiles, which showed an overwhelming effect of rotation. A diminishing in R_v due to a decrease in Ω is because of the presence of gravitational and Lorentz force rotating at very low speeds. This indicates that a friction factor is noticed, hence R_v decreases. The same trend is apparent in Figs. 16 and 17, which represented velocity and temperature profiles for different values of P_r. Prandtl number can be defined as the ratio of momentum diffusivity to thermal diffusivity. It is, therefore, obvious that a lower thermal conductivity material leads to high velocity and a different trend is seen for higher thermal conductivity. Hence, in Fig. 17, it is seen that an increase in Prandtl number accelerates the resultant velocity profiles. Likewise, in Figs. 16, an increase in P_r reduces the thermal boundary layer thickness and average temperature within the boundary. This implies that, an increase in P_r makes the thermal conductivity of the fluid to increase. Thus, resulting in rapid diffusivity of the heated surface.

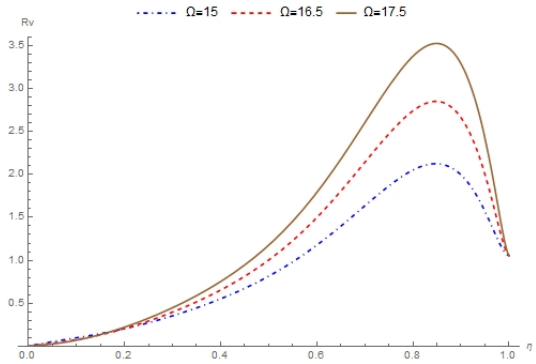

Fig. 15 Variation of resultant velocity R_v with rotation parameter Ω

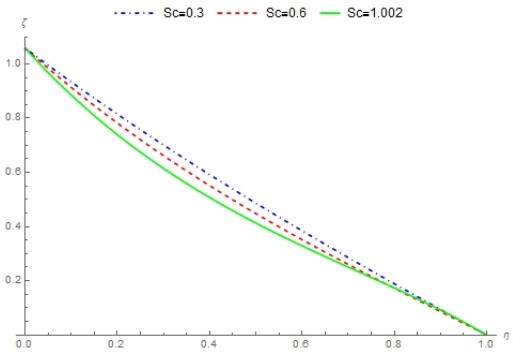

Fig. 18 Variation of dimensionless concentration ζ with Schmidt number Sc

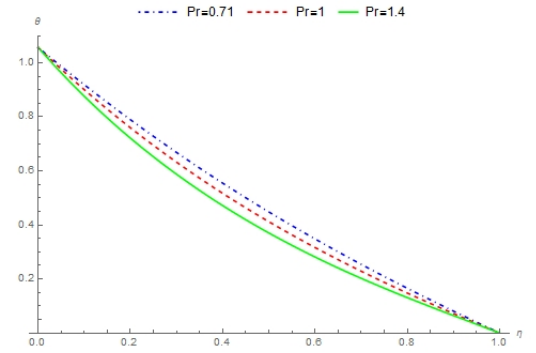

Fig. 16 Variation of dimensionless temperature ϑ with Prandtl number Pr

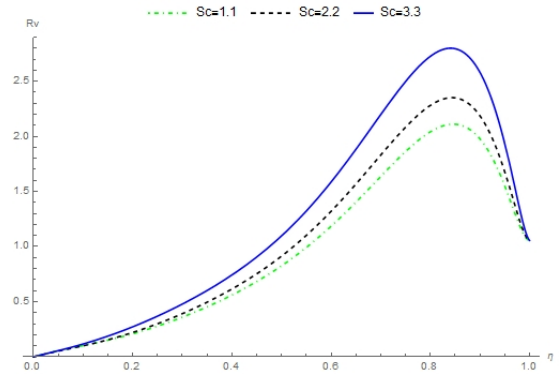

Fig. 19 Variation of resultant velocity R_v with Schmidt number Sc

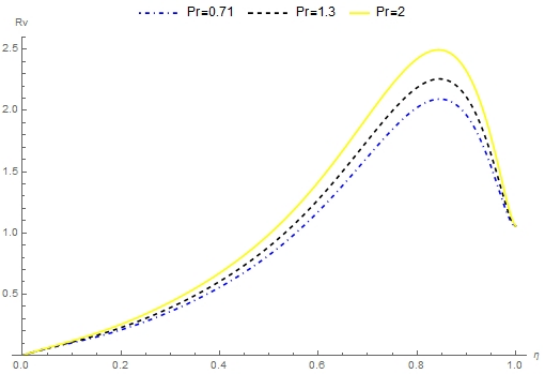

Fig. 17 Variation of resultant velocity R_v with Prandtl number Pr

Furthermore, effect of S_c on concentration and resultant velocity profiles is revealed in Figs. 18 and 19. Here, it is observed that higher Sc leads to a decline in concentration profiles, while the resultant velocity is enhanced.

Figure 20 depicts the variation of different values of heat absorption coefficient (ϕ). It is seen that with a rise in ϕ, the temperature diminishes. Thus, when heat is absorbed, the buoyancy force decreases the temperature profile. Effect of V_R on resultant velocity is displayed in Fig. 21. It is evident in Fig. 21 that resultant velocity is accelerated by an increase in V_R.

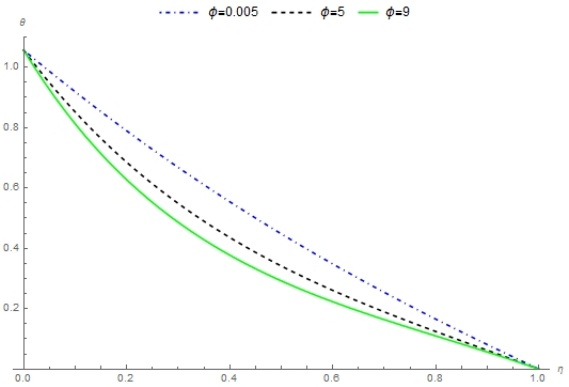

Fig. 20 Variation of dimensionless temperature ϑ with heat absorption coefficient ϕ

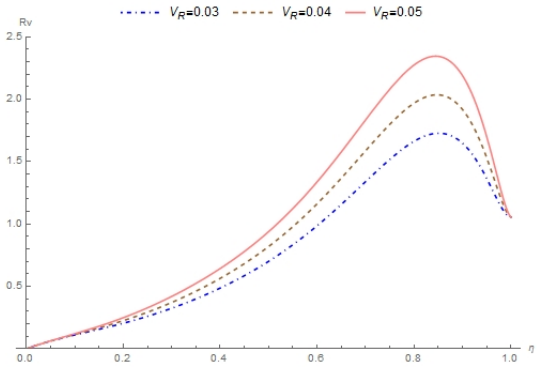

Fig. 21 Variation of resultant velocity R_v with dimensionless viscoelasticity parameter of the Rivlin-Ericksen fluid V_R

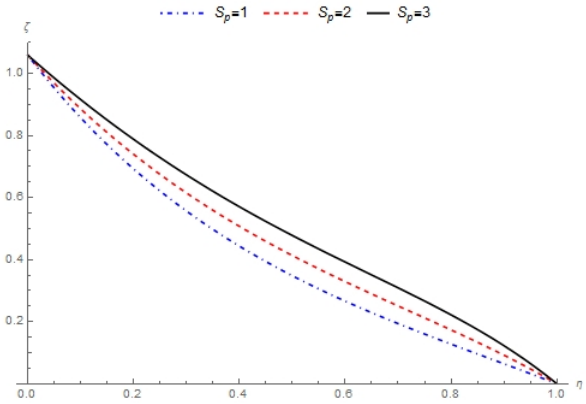

Fig. 24 Variation of dimensionless concentration ζ with Soret parameter S_p

Figures 22 - 24 detect the effects of variation of S_p on resultant velocity, temperature and species profiles. A careful study of these figures shown that the presence of S_p enhances both resultant velocity and concentration profiles, while a different trend is noticed in temperature profiles. Temperature profiles decline with a rise in S_p.

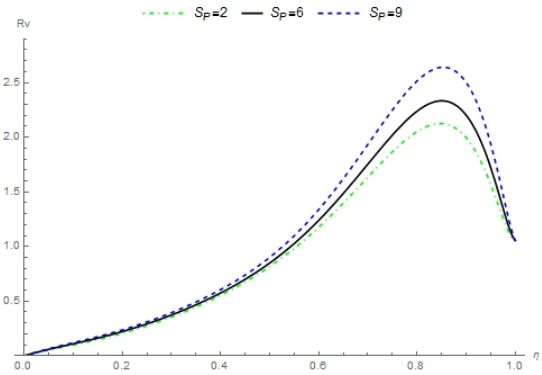

Fig. 22 Variation of resultant velocity R_v with Soret parameter S_p

Effect of D_p on resultant velocity, temperature and concentration profiles is presented in Figs. 25 - 27. Resultant velocity profiles diminishes as D_p is increased, while temperature profiles increases. This is as a result of the generation of energy flux that enhances the temperature. A rise in D_p makes concentration profiles to fall within $0 \leq \eta \leq 0.7$. and within $0.7 \leq \eta \leq 1$, a rise in concentration profile is observed.

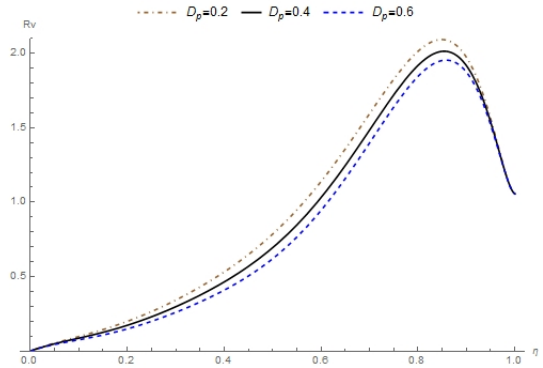

Fig. 25 Variation of resultant velocity R_v with Dufour parameterD_p

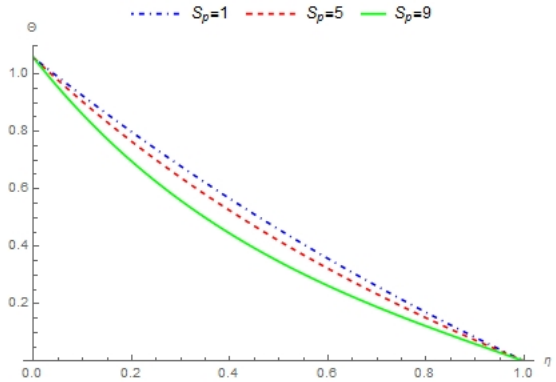

Fig. 23 Variation of dimensionless temperature ϑ with Soret parameter S_p

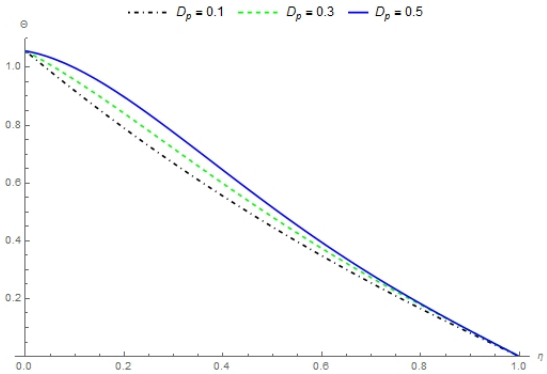

Fig. 26 Variation of dimensionless temperature ϑ with Dufour parameter D_p

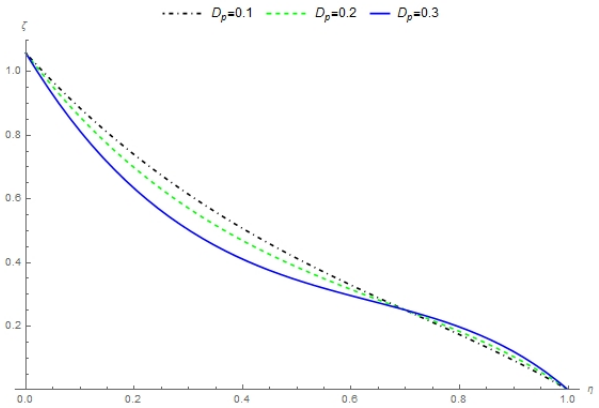

Fig. 27 Variation of dimensionless concentration ζ with Dufour parameter D_p

Tables 1 and 2 display the variation of fluid parameters (K_r, E, Ω, S_p, D_p and V_R) on Skin-friction, Nusselt number and Sherwood Number at $\eta = 0$ and $\eta = 1$. It is seen in Table 1 that the Skin-friction is diminished with the presence of K_r, Ω, D_p and V_R, while it is strengthened by E and S_p. Nusselt number is reduced with an increase in K_r, N, and D_p. On the other hand, increasing the values of S_p enhances the Nusselt number. In like manner, Sherwood number increases with an increase in chemical reaction and Dufour parameter. The mass transfer coefficient value is reduced with an increase in E and S_p. Consequently, Table 2 shows that skin friction is quickened by an increase in K_r, E, Ω, S_p and V_R, while higher values of Dufour parameter decreases the Skin-friction. Nusselt number is risen with an increase in K_r and D_p but diminishes with increment in the values of E and S_p. Increasing E, S_p and D_p make Sherwood number to rise and it decelerates by increasing the values of K_r.

Table 1 Values of Skin-friction, Nusselt number and Sherwood Number for different parameters at $\eta = 0$

K_r	E	Ω	S_p	D_p	V_R	τ	Nu	Sh
1	3	15	2	0.1	0.05	1.26547	2.11822	1.51979
2	3	15	2	0.1	0.05	1.23144	2.05517	1.88701
3	3	15	2	0.1	0.05	1.20171	1.99740	2.21109
2	2	15	2	0.1	0.05	1.22856	2.24886	2.02036
2	3	15	2	0.1	0.05	1.23144	2.05517	1.88701
2	4	15	2	0.1	0.05	1.23326	1.95820	1.80325
2	3	10	2	0.1	0.05	2.30656	2.05517	1.88701
2	3	12	2	0.1	0.05	1.91408	2.05517	1.88701
2	3	14	2	0.1	0.05	1.47608	2.05517	1.88701
2	3	15	0.5	0.1	0.05	1.15877	1.96696	2.39242
2	3	15	1	0.1	0.05	1.18374	1.99150	2.23485
2	3	15	1.5	0.1	0.05	1.20808	2.02105	2.06581
2	3	15	2	0.2	0.05	1.23902	1.91244	2.24897
2	3	15	2	0.3	0.05	1.22160	1.68476	2.84090
2	3	15	2	0.4	0.05	1.17973	1.28395	3.77168
2	3	15	2	0.1	0.03	1.88677	2.05517	1.27000
2	3	15	2	0.1	0.04	1.24755	2.05517	1.88689
2	3	15	2	0.1	0.05	1.23144	2.05517	1.88701

Table 2 Values of Skin-friction, Nusselt number and Sherwood Number for different parameters at $\eta = 1$

K_r	E	Ω	S_p	D_p	V_R	τ	Nu	Sh
1	3	15	2	0.1	0.05	31.07010	1.11707	1.01404
2	3	15	2	0.1	0.05	31.18150	1.15218	1.00215
3	3	15	2	0.1	0.05	31.30150	1.18574	0.99255
2	2	15	2	0.1	0.05	30.93190	1.39006	0.92341
2	3	15	2	0.1	0.05	31.18150	1.15218	1.00215
2	4	15	2	0.1	0.05	31.34460	1.03570	1.05271
2	3	10	2	0.1	0.05	10.07210	1.15218	1.00215
2	3	12	2	0.1	0.05	15.89760	1.15218	1.00215
2	3	14	2	0.1	0.05	31.18150	1.15218	1.00215
2	3	15	0.5	0.1	0.05	30.56020	1.17756	0.51807
2	3	15	1	0.1	0.05	30.73410	1.17484	0.66103
2	3	15	1.5	0.1	0.05	30.94190	1.16610	0.82349
2	3	15	2	0.2	0.05	30.65410	1.20466	1.20452
2	3	15	2	0.3	0.05	30.07210	1.25950	1.47638
2	3	15	2	0.4	0.05	29.37250	1.29107	1.92832
2	3	15	2	0.1	0.03	22.58470	1.15218	0.99932
2	3	15	2	0.1	0.04	26.85330	1.15218	1.00074
2	3	15	2	0.1	0.05	31.18150	1.15218	1.00215

5. CONCLUSION

An investigation of the join influence of the fluid parameters on convective Rivlin-Ericksen flow of an unsteady incompressible and electrically conducting fluid in vertical plates with a time dependence suction is discussed. The governing equations of the flow field were non-dimensionalised and the solutions are obtained using Adomian decomposition method. The effects of various parameters on velocity, temperature, concentration, skin friction, Nusselt number and Sherwood number are presented in graphical and tabular forms.
The study reveals that;

1. Resultant velocity is strengthened by the presence of Ω, E, V_R, and S_p and weakened with the presence of K_r and D_p.

2. An increase in D_p tends to accelerate temperature profiles, while it is slowed down by higher values of E and S_p.

3. Concentration distribution is enhanced with increase in S_p, however, the profile is reduced with an increase in K_r and D_p. Within $0.7 \leq \eta \leq 1$, higher values of D_p improved the profile.

4. Skin friction is enhanced with an increase in the values of S_p and decelerated by increasing D_p and Ω at $\eta = 0$. The same effect is noticed for S_p and D_p at $\eta = 1$. But, Ω tends to accelerate the skin friction.

5. At $\eta = 0$, it is observed that increasing in the Soret number strengthens the heat transfer coefficient and weakens mass transfer coefficient. The reverse effect is noticed for Dufour number.

6. Both heat and mass transfer coefficients are improved by high values of D_p at $\eta = 1$.

NOMENCLATURE

x^* dimensional distance upward the plate (m)
y^* dimensional distance normal to the plate (m)
z^* dimensional distance perpendicular to the planes of the plates (m)
u^*, v^*, w^* dimensional velocity components in the x^*, y^*, z^* directions respectively (ms^{-1})
t^* dimensional time (s)

C_p	specific heat at constant pressure ($\mathrm{Jkg^{-1}K^{-1}}$)
B_0	magnetic induction (tesla)
T^*	dimensional temperature (K)
C^*	dimensional concentration ($\mathrm{kmol/m^3}$)
P^*	dimensional pressure ($\mathrm{N/m^2}$)
D	chemical molecular diffusivity
g	gravitational acceleration ($\mathrm{m/s^2}$)
T_h^*	plate dimensional temperature (K)
C_h^*	plate dimensional concentration ($\mathrm{kmol/m^3}$)
k_p	non-dimensional permeability of the porous medium
$k^{'}$	mean absorption coefficient
W_o	scale of suction velocity contain non-zero positive constant
T_m	mean fluid temperature
K_T	thermal diffusion ratio
C_s	concentration susceptibility
K	thermal conductivity ($\mathrm{W/m \cdot K}$)
T_0	temperature at the left plate (K)
C_0	concentration at the left plate ($\mathrm{kmol/m^3}$)
h	distance of the plate (m)
Greek Symbols	
ρ^*	fluid density ($\mathrm{kgm^{-3}}$)
ν^*	kinematic viscosity ($\mathrm{m^2s^{-1}}$)
σ	Stefan-Boltzman constant ($\mathrm{W/m^2 \cdot K^4}$)
ϕ_o	dimensional heat absorption coefficient (j/kg)
α	thermal diffusivity
β_T,β_C	thermal, concentration expansion coefficient
β_1	kinematic viscoelasticity
ϵ	scalar constant

REFERENCES

Abdulmaleque, K.L., 2017, "Temperature dependent suction/injection and variable properties on non-Newtonian Casson mixed convective MHD laminar fluid flow with viscous dissipation and thermal radiation," *American Journal of Heat and Mass Transfer*, **4**(2), 104–120. http://dx.doi.org/10.7726/ajhmt.2017.1007.

Aruna, G., Varma, S.V., and Raju, R.S., 2015, "Combined influence of Soret and Dufour effects on unsteady hydromagnetic mixed convective flow in an accelerated vertical wavy plate through a porous medium," *Int J Adv Appl Math and Mech*, **3**(1), 122–134.

Babu, H.D., Venkateswarlu, B., and Narayana, S.P.V., 2017, "Soret and Dufour effects on MHD radiative heat and mass transfer flow over a stretching sheet," *Frontiers in Heat and Mass Transfer(FHMT)*, **8**(5), 1–9.
http://dx.doi.org/10.5098/hmt.8.5.

Beard, D.M., and Walters, K., 1964, *Elastico-viscous boundary-layer flows-I: two-dimensional flow near the stagnation point*, Proc. Cambr. Phil. Soc., London.

Brewster, M.Q., 1972, *Thermal Radiation Transfer Properties*, John Wiley and sons, London.

Dada, M.S., and Agunbiade, S.A., 2016, "Radiation and chemical reaction effects on convective Rivlin-Ericksen flow past a porous vertical plate," *Ife Journal of Science*, **18**(3), 655–667.

Dada, M.S., and Salawu, S.O., 2017, "Analysis of Heat and Mass Transfer of an inclined magnetic field pressure-driven flow past a permeable plate," *Applications and Applied Mathematics: An international Journal (AAM)*, **12**(1), 189–200.
http://pvamu.edu/aam.

Das, S., Maity, M., and Das, J.K., 2011, "Effect of heat source and variable suction on unsteady viscous stratified flow past a vertical porous flat moving plate in the slip flow regime," *International Journal of Energy and Environment*, **2**(2), 375–382.

Deepthi, J., and Prasada, D.R.V., 2017, "Mixed convective heat and mass transfer flow in a vertical channel with Soret effect and radiation," *International Journal of Emerging Trends in Engineering and Development*, **2**(7), 1–11.
http://www.rspublication.com/ijeted/ijeted index.htm.

Devasena, Y., and Ratmat, A.L., 2014, "Effect of thermo-Diffusion on mixed convective Heat and mass transfer flow of a Visco-Elastic fluid past a porous plate with Heat Generating Sources," *International Journal of Emerging Trends in Engineering and Development*, **2**(4), 8–19.
http://www.rspublication.com/ijeted/ijeted$_index.htm$.

Garg, B.P., Singh, K.D., and Bansal, A.K., 2014a, "An oscillatory MHD convective flow of viscoelastic fluid through porous medium filled in a rotating vertical porous channel with heat radiation," *International Journal of Engineering and innovative Technlolgy*, **3**(12), 273–281.

Garg, B.P., Singh, K.D., and Bansal, A.K., 2014b, "Rotating MHD convective flow of Oldroyd-B fluid through a porous medium in a vertical porous channel with thermal Radiation," *International Journal of Innovations in Engineering and Technology*, **4**(1), 251–267.

Gbadeyan, J.A., Idowu, A.S., Ogunsola, A.W., Agbola, O.O., and Olarewaju, P..O., 2011, "Heat and mass transfer for Soret and Dufour's effect on mixed convection boundary layer flow over a stretching vertical surface in a porous medium filled with a viscoelastic fluid in the presence of magnetic field," *Global Journal of Science Frontier Research*, **11**(8), 96–115.

Guria, M., and Jana, R.N., 2013, "Flow of a viscoelastic fluid past a porous plate in a rotating system," *Int J of Applied Mechanics and Engineering*, **18**(1), 27–41.
http://dx.doi.org/10.2478/ijame-2013-0002.

Hayat, T., Zahir, H., Tanveer, A., and Alsaedi, A., 2017, "Soret and Dufour effects on MHD peristaltic transport of Jeffrey fluid in a curved channel with convective boundary conditions," *PLoS ONE*, **12**(2), 1–50.
http://dx.doi.org/10.1371/journal.pone.0164854.

Ibrahim, S.M., and Suneetha, K., 2015, "Chemical reaction and Soret effects on unsteady MHD flow of a viscoelastic fluid past an impulsively started infinite vertical plate with heat source/Sink," *International journal of Mathematics and conputational Science*, **1**(1), 5–14.
http://www.publicscienceframework.org/journal/ijmcs.

Jimoh, A., Idowu, A.S., and Titiloye, E.O., 2014, "Influence of Soret on unsteady MHD of Kuvshinshiki fluid flow flow with heat and mass Transfer past a vertical porous plate with vertical suction," *International journal of Recent and Innovation Trends in computing and communication*, **2**(9), 2599–2611.
http://www.ijritcc.org.

Mutua, N.M., Musyoki, N.M., Kinyanjui, M.N., and Kwanza, J.K., 2013, "Magnetohydrodynamic free convection flow of a heat generating fluid past a semi-infinite vertical porous plate with variable suction," *International Journal of Applied Mathematics Research*, **2**(3), 356–371.

Reddy, P.C., Raju, M.C., and Raju, G.S.S., 2016, "Soret and Dufour effects on MHD free convective flow of Rivlin-Ericksen fluid past a semi-infinite vertical plate," *Advances and Applications in Fluid Mechanics*, **19**(2), 401–414.
http://dx.doi.org/10.17654/FM019020401.

Sarma, G.S., and Govardhan, K., 2016, "Thermo-diffusion and Diffusion-thermo effects on free convective heat and mass transfer from vertical surface in a porous medium with viscous dissipation in the presence of Thermal radiation," *Archives of Current Research International*, **3**(1), 1–11.
http://dx.doi.org/10.9734/ACRI/2016/21503.

Sibanda, P., and Makinde, O.D., 2010, "On steady MHD flow and heat transfer due to a rotating disk in a porous medium with ohmic heating and viscous dissipation," *Int J Num Methods for Heat and Fluid Flow*, **20**(3), 269–285.

Singh, K.D., 2013, "Visco-Elastic MHD convective periodic flow through porous medium in a rotating vertical channel with thermal radiation," *Journal of Global Research in Mathematics Archives*, **1**(4), 8–20.
http://www.jgrma.info.